❒　　4820

In-wheel, outer rotor, permanent magnet synchronous motor design with improved torque density for electric vehicle applications

Mustafa Yaseen Bdewi, Mohammed Moanes Ezzaldean Ali, Ahmed Mahmood Mohammed
Electrical Engineering Department, University of Technology, Baghdad, Iraq

Article Info	ABSTRACT
	In electric vehicle applications, the torque density of electric motor plays an important role in improving the performance of the vehicle. The main objective of this paper is to investigate a possible method for improving the torque density of a permanent magnet synchronous motor used in electric vehicles. At the same time, other machine specifications were taken into account and kept within the acceptable level. This was achieved by incorporating performance enhancement strategies such as investigating of high-efficient winding topology for the motor's stator to give the highest winding factor and optimizing the machine dimensions to achieve the best performance. MagNet 7.4.1 software package with static and transient finite element method solver was used for implementing the proposed design. The results showed a significant improvement in the torque density with keeping the overall machine performance.
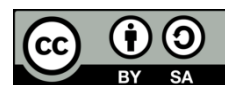
Corresponding Author:

Mustafa Yaseen Bdewi
Electrical Engineering Department, University of Technology
Baghdad, Iraq
Email: 316539@student.uotechnology.edu.iq

1. INTRODUCTION

Permanent magnet synchronous motor (PMSM) is a type of motors that uses permanent magnet (PM) for producing the necessary rotor excitation field. PMSMs are widely employed in electric vehicles (EVs) due to their attractive properties in terms of reliability, compactness, power density and efficiency, where this motor has the highest efficiency and power density among other types of electric motors. By using the PMs, the DC supply for excitation is no longer required. Moreover, eliminating copper from the rotor allows the motor design with smaller rotor diameters resulting in lower rotor inertia [1]–[6]. Two techniques may be used in EV drives to achieve high efficiency and power density. The first technique depends on higher speed motors for the same output power rate in order to reduce the volume and weight. However, gear and clutch are required in this technique which adds mechanical losses during transmission of power from the motor to the wheels. Another technique includes the usage of low-speed, high-torque motors that is directly connected to the wheels. This arrangement is called in-wheel motor. Power transfer equipment such as gear can be removed, therefore the transmission loss is minimized, and the efficiency of operations is improved. Also, regeneration braking occurs in each wheel that prolongs the driving distance. The modern EV with in-wheel motor has many other benefits such as fast torque response and individual control of each wheel [7], [8]. This drive kind also provides advanced vehicle dynamic control technologies such as anti-lock brake system (ABS), electronic stability program (ESP) and electronic brake force distribution (EBD) [9].

Conventionally, PMSMs, for traction drives, are designed with inner rotor models while motors of outer rotor are mainly limited to applications which benefit from the direct connection between the traction drive and the rotor surface. Recently, outer rotor motors have been marketed for traditional traction applications as they develop higher torque density in comparison with inner rotor PMSMs [10]. The torque is produced at a diameter which is large relative to the motor diameter, i.e., the same torque can be developed by means of lower magnetic and electric loading compared with that of inner rotor permanent magnet motor. Also, PMSM with outer rotor has the merit of higher inertia due to its larger air gap [11].

In EVs, electric motor with high power/torque density is highly recommended [12], [13]. In [14], the improvement of the torque density (torque/weight) by machine dimensions' optimization was implemented by variation the rotor diameter of the investigated machine. In [13], the use of innovative screen printed winding and innovative materials, such as iron cobalt was investigated for improving the torque density. In [15], measures to design an outer rotor PMSM with improved torque density were proposed, involving the usage of high-performance laminated material, open slots, unequal teeth widths, and Halbach arrays. In [16], the torque density enhancement was proposed by variation the stator teeth and tips width for motors with similar slots and poles combinations. In [17], a ring shape PMs and toroidal concentrated winding with soft magnetic composite core were suggested for improving the torque density. However, most of previous studies about improving the torque density of PMSM ignore the change that may occur on the torque ripple and neglect the effect of one or both of the magnetic saturation and demagnetization of PM.

In this paper, the multi-objective optimization technique is used to increase the torque density and preserve low torque ripple with considering both of magnetic saturation and demagnetization effects. The proposed method is implemented according to the following stages: i) investigating of highly efficient arrangement for the stator winding, ii) selecting the appropriate materials of permanent magnet and laminated steel, and iii) optimizing the machine dimensions including slot opening, slot width and magnet span.

In this work, the mathematical analysis is based entirely on finite element method (FEM) is used which provides high computational accuracy. This paper is arranged as follows: section 2 describes the research method. Section 3 shows results and discussions. Section 4 presents the conclusion.

2.   RESEARCH METHOD

In this section, the motor specifications are explained to select an appropriate design model based on electromagnetic torque, cogging torque, vibration, and magnetic noise. Then, motor materials are explained to select a suitable PM, stator, and rotor material types for PMSM. Finally, the machine sizing is explained to show the geometries effect on the motor performance for optimizing the machine according to the desired specifications.

2.1. Design specifications

In permanent magnet synchronous motors, there are various slot/pole (Q_s/p) combinations which are affecting the machine electromagnetic torque, cogging torque, vibration, and magnetic noise [18]. The electromagnetic torque is influenced by the winding factor (k_w) for each combination. The higher the fundamental winding factor, the higher back electromotive force (EMF) and thus higher torque [19]. The winding factor can be expressed as (1) [18]:

$$k_w = \frac{\sum_{i=1}^{2Q_s/3} EMF_i}{n_l Q_s/3} \tag{1}$$

where (i) is the number of winding conductors, and (n_l) is the number of layers. Motors with low winding factor use the winding turns ineffectively and therefore have a low torque. Thus, it is essential to select a slot/pole combination having high winding factor [18]. The other factor is cogging torque which is produced by the interaction between the PM poles with the stator [1]. Cogging torque is symmetrically fluctuated and number of cogging cycles per one revolution (N_{ct}) is equal to the least common multiple (LCM) of slots number and poles number and it is equal to (2) [19]:

$$N_{ct} = LCM(Q_s, P) \tag{2}$$

Since the cogging torque value is inversely proportional to the cogging cycles, higher number of cogging cycles is desired. The cogging torque has a fundamental frequency and sub-harmonics, so the cogging torque can be modelled as a summation of the fundamental and the higher order harmonics as (3) [19]:

$$T_{ct} = \sum_{n=1}^{\infty} T_{ctn} \sin(nN_{ct}\theta + \phi_n) \tag{3}$$

where (n) is the harmonic order, (T_{ctn}) is the maximum cogging torque of (n) order, (θ) is the rotational angle, and (φ_n) is (n) order phase shift.

The stator winding can be wounded as concentrated or distributed winding. In this work, concentrated winding is employed due to its advantages in comparison with the distributed winding. These advantages include higher power density, lower cogging torque, shorter end winding, better flux weakening capability, and higher slot fill factor [20]. The investigated winding topology and its layout techniques are detailed in [18].

Symmetry of machine sections is also one of the significant factors that affects the selection of slot/pole combination. Machine winding with unsymmetrical sections (e.g., Q_s=6k+9 where k=0,1,2 ..., and p=Q_s±1) has high unbalanced radial forces. Winding with more symmetrical periods gives the best performance and avoids unwanted vibration and noise [18]. According to the previous considerations, 72 slot/60 pole combination has been selected. This combination gives high winding factor (0.933), high LCM and six sections of symmetry which are desirable for EV applications. Figure 1 shows the investigated PMSM, Figure 1(a) displays the general view of the motor and Figure 1(b) illustrates the suggested configuration of the winding. Only a section of one sixth of the winding configuration is appeared in the figure and the other five sections are symmetric to this section. The specifications of the initial design and the geometry parameters which is based on work presented in [21] are displayed in Table 1.
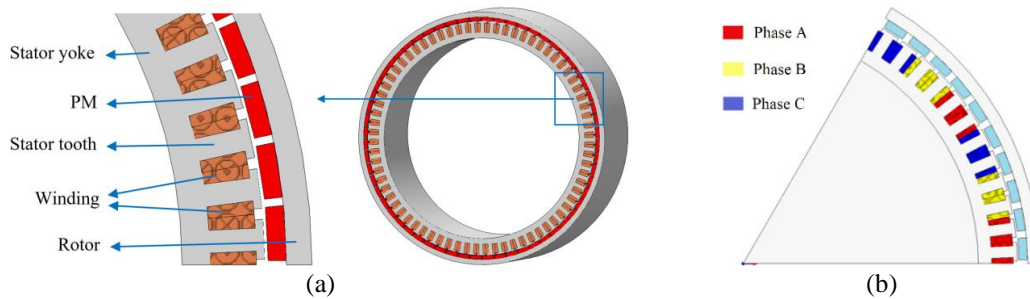

Figure 1. The investigated PMSM (a) general view and (b) the winding configuration

Table 1. The initial design parameters of the PMSM [21]

Parameter	Value	Parameter	Value
Rated current density (A/mm^2)	5	Rotor inner radius (mm)	252.1
Rated speed (rpm)	500	Rotor yoke thickness (mm)	11
Conductor diameter (mm)	2.5	Magnet thickness (mm)	7.9
Machine weight (kg)	158	Magnet span (%)	88.4
Outer radius (mm)	271	Stator yoke thickness (mm)	12
Inner radius (mm)	215	Slot width (mm)	10.4
Stack length (mm)	272	Slot opening (%)	39.2
Air gap length (mm)	1.5		

The investigated motor is surface mounted PM model which has simpler construction and lower cost compared with embedded PM model [22]. According to static computations, the embedded magnet rotor gives larger torque compared with surface mounted magnet rotor. However, according to dynamic analysis, it has been shown that the embedded magnet gives slightly less electromagnetic torque [23]. Due to the usage of an outer rotor structure, the wheel speed is equal to the motor speed. The motor rated speed is 500 rpm which determined by considering the vehicle rated speed, the wheel outer diameter and the limitations of inverter size and iron losses. The higher motor rated speed, the higher iron losses, and inverter size. The rated current density is determined in accordance with the cooling mechanism of the motor. Considering that the air-cooling method is used, the value of rated current density is determined as (5 A/mm^2) [24].

2.2. Materials selection

In PM motors design, the selection of PM type is influenced by the kind of application, and economical considerations. For high torque density machines, permanent magnets made from alloys of rare earth elements are utilized due to their interesting properties. Rare earth materials involve two different types: NdFeB and SmCo. These kinds of PMs are widely used in PMSMs due to their good magnetic characteristics and cost reduction [25], [26]. For the investigated design, NdFeB type 38/15 PM has been selected due to its

cons in terms of characteristics, performance, and cost. For the core of stator and rotor, there are two basic properties have to be considered involving the B-H curve and the iron losses [11]. Solid material or laminated material can be used for the core structure of the machine [27]. Laminated low silicon, soft alloy steel has been selected to construct the stator and rotor core. The thinner the laminated material, the lower the iron losses, but higher cost [11]. Figure 2 displays the magnetic characteristics of different laminated steel materials [28], Figure 2(a) shows the variation of the magnetic flux density (B) with the magnetic field intensity (H), and Figure 2(b) shows the variation of the loss density with the magnetic flux density.

In this work, M350-50A laminated steel of 0.5 mm thickness is used owing to its high saturation flux density (1.8 T) and relatively low loss density. Figure 3 shows the B_{peak}– loss density of M350-50A at different frequencies. Here, it can be seen that the losses increase with increasing the frequency and the flux density [28].
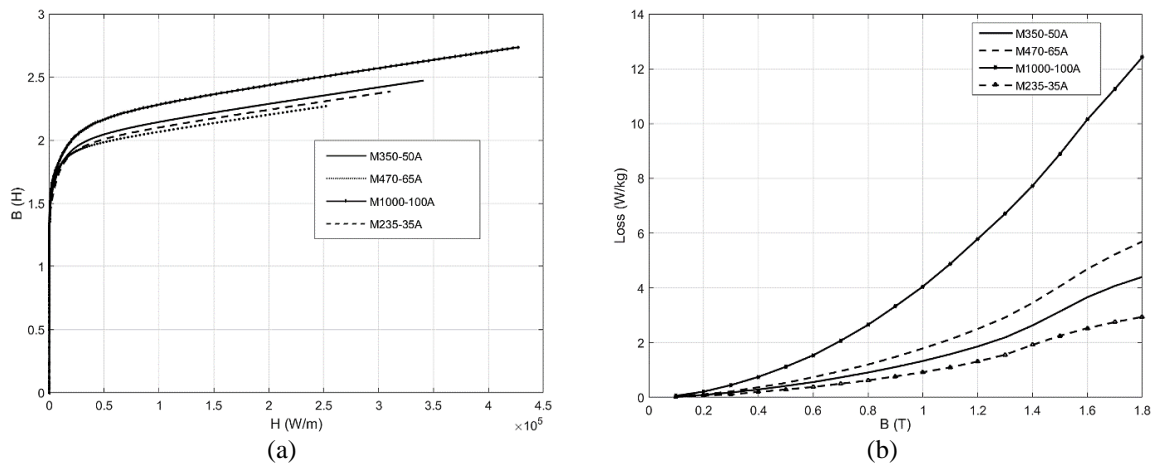

(a)   (b)

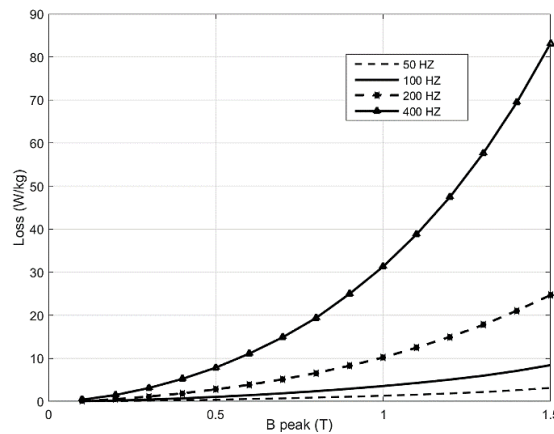Figure 2. Typical magnetic characteristics of steel alloys (a) B-H curves and (b) losses [28]

Figure 3. B_{peak}-loss density curves of M350-50A at different frequencies [28]

2.3. Machine sizing

The physical size of machines is primarily affected their torque capability. The electromagnetic torque is proportional to the product of the shear stress (σ), rotor diameter (D), and stack length (L). In turn, the shear stress is proportional to the product of electric and magnetic loading. The equation of electromagnetic torque can be expressed as (4) [29]:

$$T_e = \frac{\pi}{2} D^2 L \sigma \qquad (4)$$

The magnetic loading is normally limited by saturation of the stator teeth and hence by the flux density and the stator tooth width to the tooth spacing ratio. The electrical loading is also constrained by many factors

including the stator slot depth, winding fill factor, and the permissible current density [24], [29]. The poles number of the machine is limited by the desired synchronous speed. This restriction is no longer applied to the inverter driven PMSMs as the inverter can produce any desirable frequency. Higher number of poles considerably reduces the thickness of stator and rotor yoke. However, the pole number also increases the iron losses and PMs eddy current losses and decreases the winding inductance. The physical air-gap length of the machine is made as small as possible to save an amount of permanent magnet material. This is applied specially for low-speed high torque PM machine [24]. However, very small airgap is not practical because of the vibration and the manufacturing constraints. Thus, the air-gap length will be kept constant for the proposed design. The motor is integrated with the vehicle wheel, so the outer diameter is restricted by the wheel size. In order to enhance the machine torque density, dimensions including magnet span, slot opening, and slot width have been optimized. These three dimensions is selected to be optimized due to their major influence on the machine performance. The variable dimensions of the motor and their ranges are shown in the Figure 4 and Table 2.

Magnet span have a lower limit to avoid weak flux density. The upper and lower limits for the slot opening are set to avoid high level of leakage flux. Slot width is selected to be equal or wider than tooth width. The wider slots width, the more turns number and thus higher torque. The maximum slot width is limited by magnetic saturation and mechanical strength of the teeth.
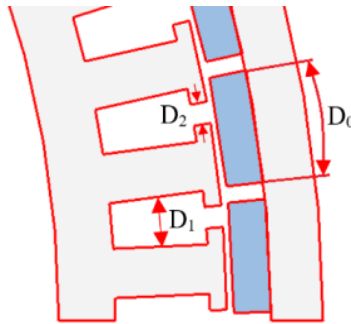

Figure 4. Variables of machine design

Table 2. Ranges of design variables [30]

Geometry	Range
Magnet span (D_0)	30-100%
Slot opening (D_2)	20-80%
Slot width (D_1)	$\geq$10 mm

2.4. Machine optimization

In high performance applications as in the case of EVs, the generated torque of PMSM should be with minimum torque ripple [31]. Torque ripple causes undesirable acoustic noises, mechanical vibrations, and shaft failure [2]. Cogging torque and the total harmonic distortion (THD) of the induced EMF are the main reasons of torque ripple [32]. Due to the direct effect of magnet shape on the air-gap flux density and EMF waveform [33], magnet span will be optimized for minimum total harmonic distortion of the air-gap flux density waveform and hence of EMF which in turn reduces the torque ripple. The THD measurement equation is given as (5) [34]:

$$THD = \frac{\sqrt{\sum_{n=2}^{\infty} B_n^2}}{B_1} \times 100\% \tag{5}$$

where B_n is the n order harmonic component of the air-gap flux density and B_1 is the fundamental component of the air-gap flux density.

Both of electromagnetic torque and torque ripple are significantly influenced by the slot opening ratio, tooth width and hence slot width [35]. Therefore, when optimizing slot opening and slot width for maximum torque density, torque ripple variation should be taken into account. During the optimization process of these parameters, the turns number of stator coils is set as variable to obtain highest possible turns number considering the actual strand area per slot. Sensitive analysis method has been used for the

optimization process to reach the target of torque density improvement using the finite element MagNet 7.4.1 and script programming Visual Basic 16.0. Also, MATLAB has been used for the THD calculation of the EMF, air-gap flux density, and electromagnetic torque.

3. RESULTS AND DISCUSSION
3.1. Optimum magnet span
Optimum magnet span can be found by studying the variation of the THD of the air-gap flux density waveform with the magnet span. This study is performed under zero percent slot opening condition to eliminate the influence of slot geometry on the distribution of the magnetic flux. Figure 5 shows the THD against magnet span. The THD is varying significantly with the magnet span because the airgap and fringing fluxes are affected by magnet span ratio. The optimal point corresponding to the minimum THD of 13.41% is at 70% magnet span. Figure 6 shows the effect of magnet span variation on the EMF waveform. It can be seen that distortion of EMF waveform is increased when the magnet span departs from the optimum ratio.
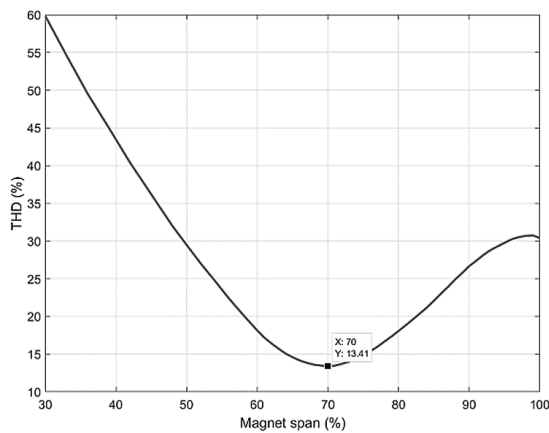

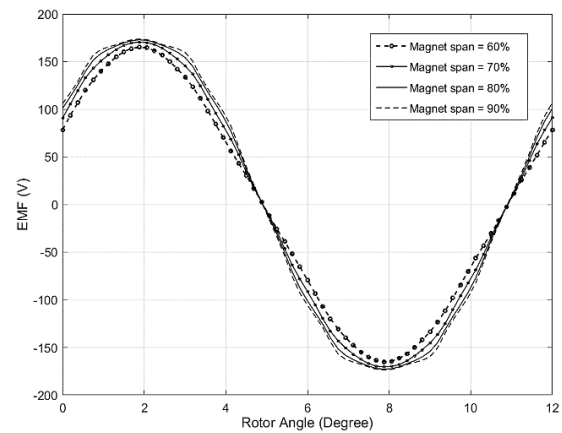Figure 5. Effect of magnet span on THD of air gap flux density waveform

Figure 6. EMF waveforms for various magnet span ratios

3.2. Optimum slot width and slot opening
Figures 7 and 8 show the effect of slot width and slot opening on the electromagnetic torque and torque ripple at rated speed and rated current density. Figures 7(a) displays the electromagnetic torque variation with the slot width, and Figure 7(b) displays the torque ripple variation with slot width at different slot opening ratios. Figure 8(a) shows the electromagnetic torque variation against slot opening, and Figure 8(b) shows the torque ripple variation against slot opening at different slot widths. It can be observed that the slot opening, and slot width have a considerable influence on the electromagnetic torque and torque ripple due to the slotting effect on the air gap flux density waveform and the reluctance variation of the magnetic circuit. The average electromagnetic torque has the maximum magnitude at the slot width and slot opening of (13.5 mm, 44%). However, if the slot width is equal or more than 12.5 mm, the teeth of the machine will be saturated since flux density exceeds 1.8 T as shown in Figure 9. Thus, the slot width practically has to be less than 12.5 mm. Considering the magnetic saturation and torque ripple, the optimum slot width and slot opening are (12.25 mm, 52%) which give an electromagnetic torque of 1636.295 Nm and torque ripple of 3.482%. As illustrated, the number of turns is variable, and it is depending on the slot width which results the turns per coil equal to 15. The final design parameters of the proposed motor are listed in Table 3.

3.3. Characteristics and parameters of the proposed motor
Figure 10 displays the electromagnetic torque characteristics obtained from the proposed motor at the rated current density and rated speed condition. The torque characteristics can be concluded from the torque curve of Figure 10(a) are illustrated in Table 4. The torque ripple has a low level of 3.482% due to the optimization of magnet span, slot width and slot opening. Figure 10(b) shows the main components of the generated torque. It can be seen that the cogging torque component appears mainly in the 12th order. Figure 11 displays the cogging torque of the proposed PMSM with a low peak to peak magnitude of 14.78 Nm. As expected, there are 12 oscillations per one electrical cycle and hence 360 oscillations per one mechanical revolution which is equal to the LCM of the number of slots and number of poles.
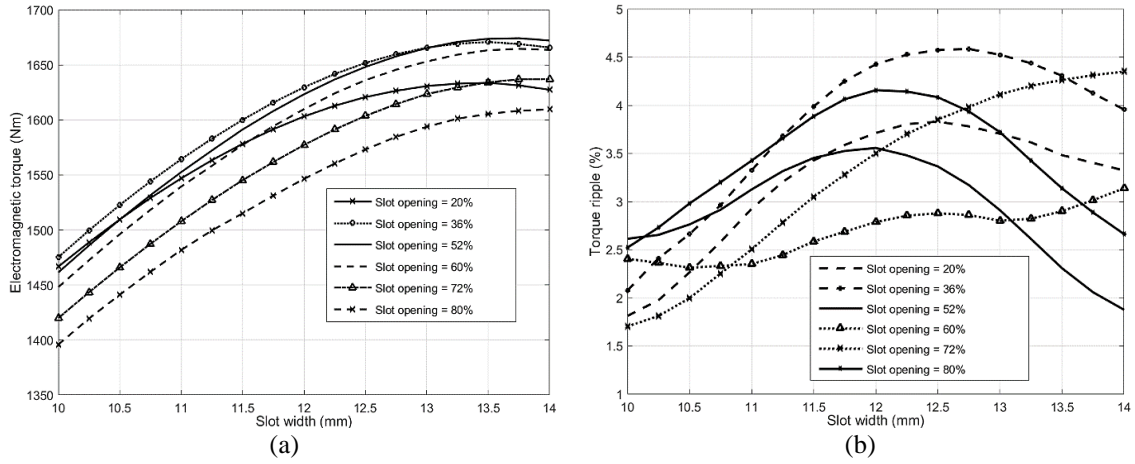
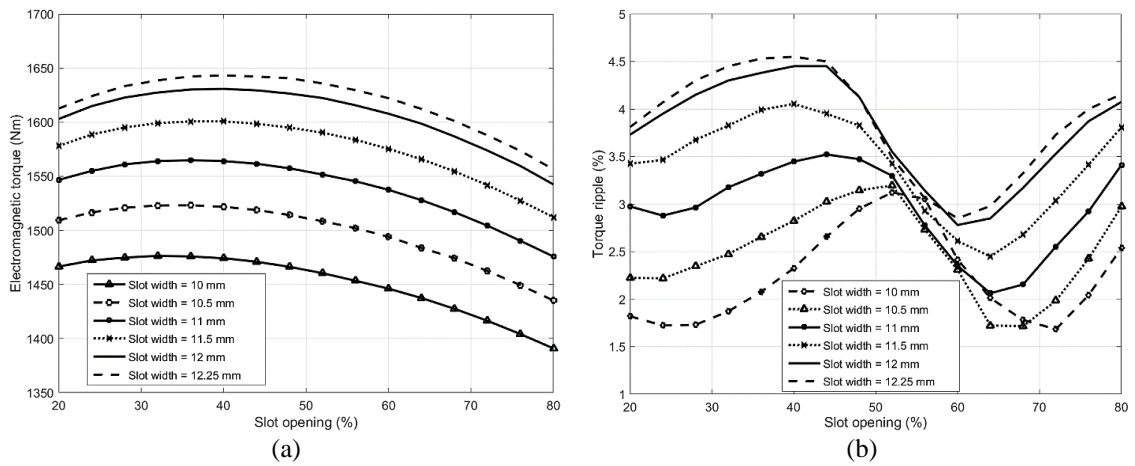Figure 7. The variation of (a) electromagnetic torque and (b) torque ripple with the slot width

Figure 8. The variation of (a) electromagnetic torque and (b) torque ripple with the slot opening
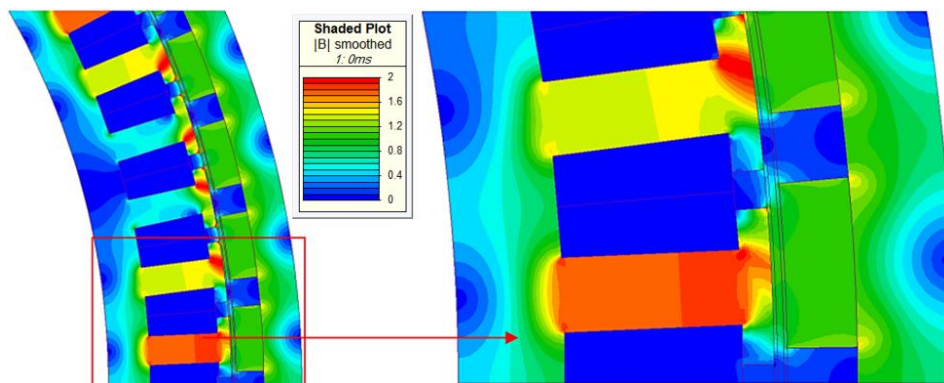

Figure 9. Flux density distribution at 12.5 mm slot width

Table 3. Final design parameters for the proposed PMSM

Parameter	Value
Magnet span (%)	70
Slot opening (%)	52
Slot width (mm)	12.25
Number of turns per coil	15
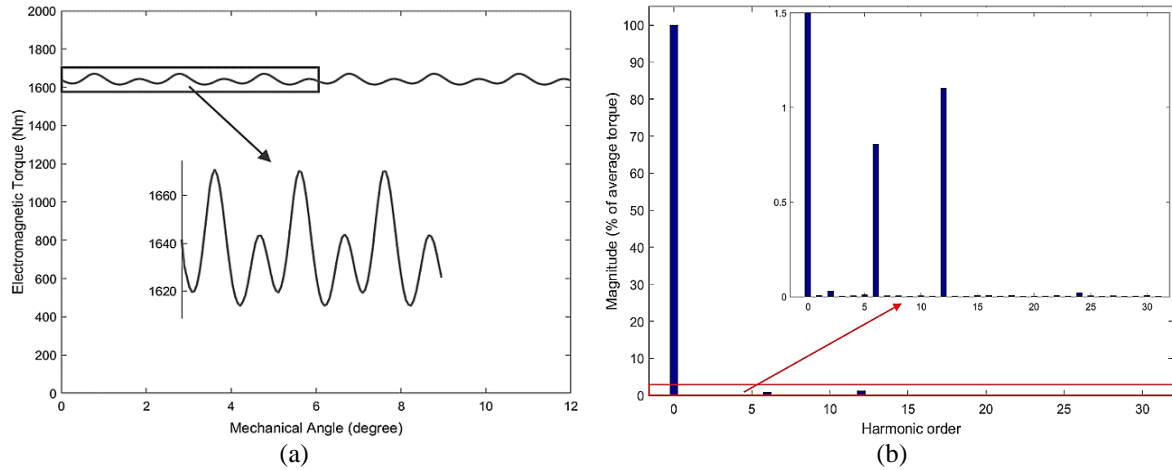
Figure 10. Electromagnetic torque at rated current density and rated speed (a) total torque and
(b) torque components

Table 4. Electromagnetic torque characteristics at rated current density and rated speed

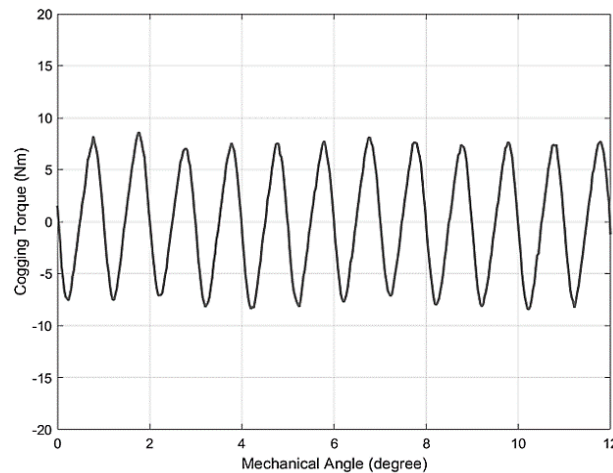| Parameters	Value
Average Torque (Nm)	1636.295
Motor weight (kg)	153.2
Torque density (Nm/kg)	10.681
Torque ripple (peak-to-peak) (Nm)	56.976
Torque ripple (%)	3.482%

Figure 11. Variation of cogging torque

Figure 12 shows the induced EMF waveforms and the harmonic spectrum of the proposed PMSM at rated speed. It is clear that the EMF has a semi-sinusoidal waveform with a low distortion as shown in Figure 12(a) which is a significant factor for the machine and the inverter. Figure 12(b) shows the harmonic spectrum of the EMF waveform from which it is observed that the third harmonic order is the highest harmonic component and THD is equal to 2.35%. Figure 13 shows the magnetic flux density and flux lines generated by PMs that linking the stator and rotor. It can be seen that the stator teeth have the highest magnetic flux density in the machine. Since the teeth do not reach the saturation level, this indicates that the performance of the proposed design is acceptable. Figure 14 displays the electromagnetic characteristics of the PMSM at overload condition of 20 A/mm^2 and rated speed. Figure 14(a) shows the electromagnetic torque variation with respect to mechanical angle. This operation condition is not practically accepted as the flux density in the stator and rotor cores reaches higher than 1.8 T which exceeds the saturation level of the material as shown in Figure 14(b). Moreover, this operation condition causes a serious increase in the

electrical losses from 2.887 kW (at rated current density) to 14.382 kW and hence, reduces the efficiency and increases the temperature of the machine.
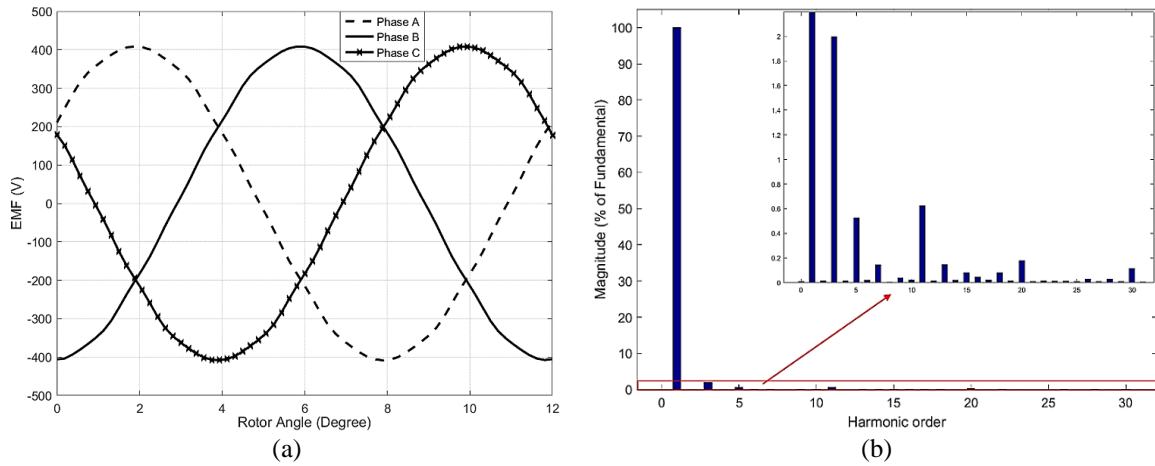

Figure 12. The motor EMF at rated speed (a) the waveforms and (b) the harmonic spectrum
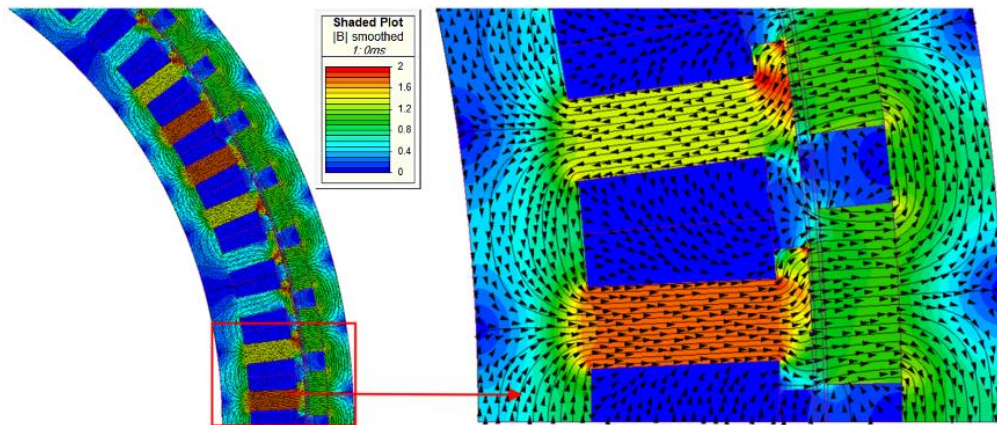

Figure 13. Flux distribution of the PMSM at rated current density and rated speed
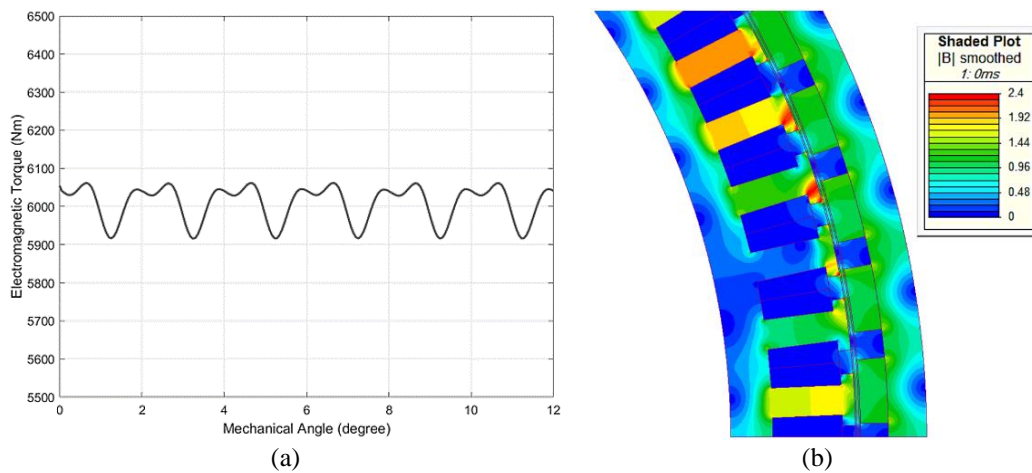

Figure 14. PMSM characteristics at overload condition (a) electromagnetic torque and (b) flux density distribution

3.4. Performance comparison of the initial and proposed permanent magnet synchronous motor (PMSM)

For illustration the significance of this work and its validity, Figure 15 compares the torque density, and torque ripple with respect to current density for the initial and proposed PMSM at rated speed. As can be seen from Figure 15(a), torque density of the proposed motor is higher than that of the initial one. Also, torque ripple of the proposed motor preserves its low magnitude as shown in Figure 15(b). At rated current density, the proposed design introduces an increment in torque density by 14.45% and percentage reduction in torque ripple by 7.39%.
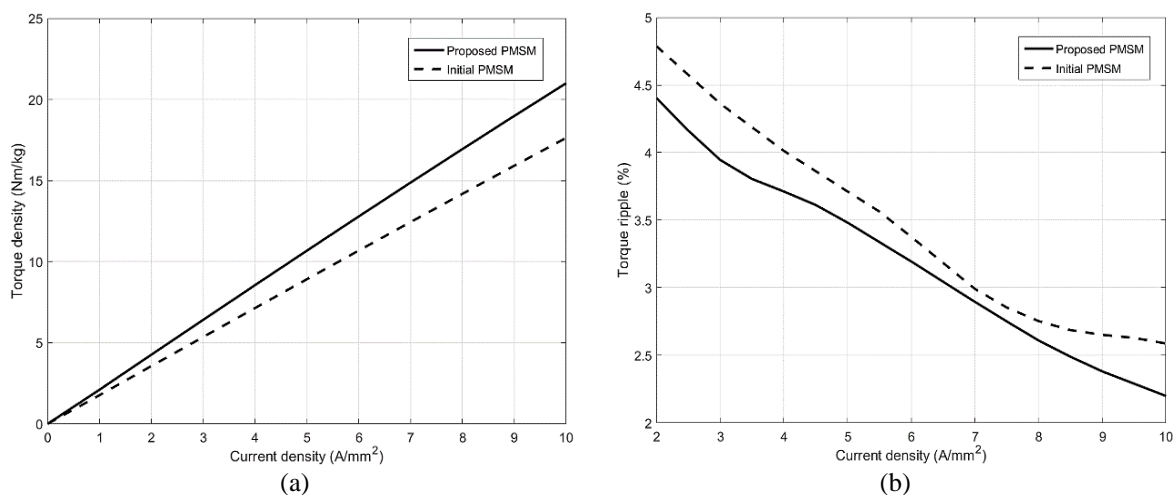

(a)

(b)

Figure 15. Comparison of the proposed and initial PMSM at rated speed (a) torque density with respect to current density and (b) torque ripple with respect to current density

4. CONCLUSION

In this paper, a design of direct drive out-runner PMSM has been investigated. In order to achieve the desired performance for electric vehicles application, a design method has been suggested which combines a set of performance improvement strategies into a well-defined structure. The work procedure started from the selection of initial design parameters, winding topology, and materials based on the desired specifications. The machine dimensions including magnet span, slot width and slot opening which have high impact on the machine performance have been altered to improve the torque density with preserving low torque ripple using sensitive optimization method and taking the overall machine performance into account. This performance improving method has been applied in a logical sequence toward the optimal electromagnetic design. By implementation the suggested procedure, the torque density performance has been improved and torque ripple is maintained with a low level at a wide range of current density, confirming the achievement of the paper goal.

REFERENCES

[1] M. Popescu, E. Tudor, S. Nicolaie, C. I. Ilie, L. Popovici, and C. Dumitru, "Experimental results regarding cogging torque reduction for the permanent magnet synchronous motors PMSM," in *2019 11th International Symposium on Advanced Topics in Electrical Engineering (ATEE)*, Mar. 2019, pp. 1–4, doi: 10.1109/ATEE.2019.8725014.

[2] J. Kim, S.-W. Ryu, M. S. Rafaq, H. H. Choi, and J.-W. Jung, "Improved torque ripple minimization technique with enhanced efficiency for surface-mounted PMSM drives," *IEEE Access*, vol. 8, pp. 115017–115027, 2020, doi: 10.1109/ACCESS.2020.3004042.

[3] D. Yadav and A. Verma, "Comperative performance analysis of PMSM drive using MPSO and ACO techniques," *International Journal of Power Electronics and Drive Systems (IJPEDS)*, vol. 9, no. 4, pp. 1510–1522, Dec. 2018, doi: 10.11591/ijpeds.v9.i4.pp1510-1522.

[4] K. R. Kumar, K. Nithin, and T. V. Kumar, "Torque ripple reduction in PMSM drive based on instantaneous voltage control technique," in *2016 IEEE 7th Power India International Conference (PIICON)*, Nov. 2016, pp. 1–6, doi: 10.1109/POWERI.2016.8077239.

[5] B. Singh, "Performance evaluation of direct torque control with permanent magnet synchronous motor," *Bulletin of Electrical Engineering and Informatics (BEEI)*, vol. 1, no. 2, pp. 165–178, Mar. 2012, doi: 10.12928/eei.v1i2.242.

[6] M. Bouazdia, M. Bouhamida, R. Taleb, and M. Denai, "Performance comparison of field oriented control based permanent magnet synchronous motor fed by matrix converter using PI and IP speed controllers," *Indonesian Journal of Electrical Engineering and Computer Science (IJEECS)*, vol. 19, no. 3, pp. 1156–1168, Sep. 2020, doi: 10.11591/ijeecs.v19.i3.pp1156-

        1168.
[7]   M. Jain and S. S. Williamson, "Suitability analysis of in-wheel motor direct drives for electric and hybrid electric vehicles," in
        2009 IEEE Electrical Power and Energy Conference (EPEC), Oct. 2009, pp. 1–5, doi: 10.1109/EPEC.2009.5420886.
[8]   A. Wojcik and T. Pajchrowski, "Torque ripple compensation in PMSM direct drive with position-based iterative learning
        control," in *2018 18th International Conference on Mechatronics - Mechatronika (ME)*, 2018, pp. 1–5.
[9]   Y. Yuan, W. Meng, X. Sun, and L. Zhang, "Design optimization and analysis of an outer-rotor direct-drive permanent-magnet
        motor for medium-speed electric vehicle," *World Electric Vehicle Journal*, vol. 10, no. 2, Apr. 2019, doi: 10.3390/wevj10020016.
[10]   A. Tovar-Barranco, F. Briz, A. Lopez-de-Heredia, and I. Villar, "Comparison of permanent magnet synchronous machines with
        concentrated windings and different rotor configurations," in *2017 19th European Conference on Power Electronics and
        Applications (EPE'17 ECCE Europe)*, Sep. 2017, pp. 1–8, doi: 10.23919/EPE17ECCEEurope.2017.8099335.
[11]   J. R. Hendershot and T. J. E. Miller, *Design of brushless permanent-magnet machines*, 2nd ed. Motor Design Books, 2010.
[12]   Y. Zhang, W. P. Cao, and J. Morrow, "Interior permanent magnet motor parameter and torque ripple analysis for EV traction," in
        2015 IEEE International Conference on Applied Superconductivity and Electromagnetic Devices (ASEMD), Nov. 2015,
        pp. 386–387, doi: 10.1109/ASEMD.2015.7453625.
[13]   M. Lindner, P. Brauer, and R. Werner, "Increasing the torque density of permanent-magnet synchronous machines using
        innovative materials and winding technologies," in *International Multi-Conference on Systems, Sygnals and Devices*, Mar. 2012,
        pp. 1–7, doi: 10.1109/SSD.2012.6198052.
[14]   T. Labbe, B. Dehez, M. Markovic, and Y. Perriard, "Torque-to-weight ratio maximization in PMSM using topology
        optimization," in *The XIX International Conference on Electrical Machines - ICEM 2010*, Sep. 2010, pp. 1–5, doi:
        10.1109/ICELMACH.2010.5608148.
[15]   M. Galea, T. Hamiti, and C. Gerada, "Torque density improvements for high performance machines," in *2013 International
        Electric Machines and Drives Conference*, May 2013, pp. 1066–1073, doi: 10.1109/IEMDC.2013.6556228.
[16]   A. Wang and Y. Tian, "A method for improving torque density in FSCW PM machines," in *2019 19th International Symposium
        on Electromagnetic Fields in Mechatronics, Electrical and Electronic Engineering (ISEF)*, Aug. 2019, pp. 1–2, doi:
        10.1109/ISEF45929.2019.9097070.
[17]   M. Ibrahim, F. Bernier, and J.-M. Lamarre, "A novel toroidal permanent magnet motor structure with high torque density and
        enhanced cooling," in *2020 IEEE Energy Conversion Congress and Exposition (ECCE)*, Oct. 2020, pp. 4044–4049, doi:
        10.1109/ECCE44975.2020.9235406.
[18]   F. Libert and J. Soulard, "Investigation on pole-slot combinations for permanent-magnet machines with concentrated windings,"
        in *International Conference on Electrical Machines (ICEM)*, 2004, pp. 5–8.
[19]   R. Krishnan, *Permanent magnet synchronous and brushless DC motor drives*, 3rd ed. CRC Press, 2017, doi:
        10.1201/9781420014235.
[20]   Z. Zhang, "Fractional slot concentrated windings interior permanent magnet traction motor with modular stator," in *2019 4th
        International Conference on Intelligent Green Building and Smart Grid (IGBSG)*, Sep. 2019, pp. 164–168, doi:
        10.1109/IGBSG.2019.8886236.
[21]   S. Bandyopadhyay, "Design optimisation of surface mounted permanent magnet synchronous motors for in-wheel electric vehicle
        applications," M.S. thesis, DC Systems, Energy Conversions and Storage, Delft University of Technology, 2015.
[22]   M. Luqman, T. C. Kwang, and A. Jidin, "Design and analysis of PM motor with semi-circle stator design using 2D-finite element
        analysis," *Indonesian Journal of Electrical Engineering and Computer Science (IJEECS)*, vol. 13, no. 1, pp. 427–436, Jan. 2019,
        doi: 10.11591/ijeecs.v13.i1.pp427-436.
[23]   P. Salminen, J. Pyrhönen, and M. Niemelä, "A comparison between surface magnets and embedded magnets in fractional slot
        wound PM motors," in *Computer Engineering in Applied Electromagnetism*, Berlin/Heidelberg: Springer-Verlag, 2006,
        pp. 209–214, doi: 10.1007/1-4020-3169-6_36.
[24]   J. Pyrhönen, T. Jokinen, and V. Hrabovcová, *Design of rotating electrical machines*. Chichester, UK: John Wiley & Sons Ltd,
        2013, doi: 10.1002/9781118701591.
[25]   I. Elosegui, M. Martinez-Iturralde, A. G. Rico, J. Florez, J. M. Echeverria, and L. Fontan, "Analytical design of synchronous
        permanent magnet motor/generators," in *2007 IEEE International Symposium on Industrial Electronics*, Jun. 2007,
        pp. 1165–1170, doi: 10.1109/ISIE.2007.4374763.
[26]   H. Muazzam, M. K. Ishak, and A. Hanif, "Compensating the performance of permanent magnet synchronous machines for fully
        electric vehicle using LPV control," *Bulletin of Electrical Engineering and Informatics (BEEI)*, vol. 10, no. 4, pp. 1923–1929,
        Aug. 2021, doi: 10.11591/eei.v10i4.2946.
[27]   A. M. Mohammed, M. Galea, T. Cox, and C. Gerada, "Consideration on eddy current reduction techniques for solid materials
        used in unconventional magnetic circuits," *IEEE Transactions on Industrial Electronics*, vol. 66, no. 6, pp. 4870–4879, Jun. 2019,
        doi: 10.1109/TIE.2018.2875641.
[28]   S. Sprague, "EMERF lamination steels third edition CD-ROM," The Motor and Motion Association, Tech. Rep., 2009.
[29]   W. Soong, "Sizing of electrical machines," *Power Engineering Briefing Notes*, vol. 9, no. 2, pp. 17–18, 2008
[30]   M. Y. Bdewi, A. M. Mohammed, and M. M. Ezzaldean, "Design and performance analysis of permanent magnet synchronous
        motor for electric vehicles application," *Engineering and Technology Journal*, vol. 39, no. 3A, pp. 394–406, Mar. 2021, doi:
        10.30684/etj.v39i3A.1765.
[31]   G. J. Li, B. Ren, and Z. Q. Zhu, "Cogging torque and torque ripple reduction of modular permanent magnet machines," in *2016
        XXII International Conference on Electrical Machines (ICEM)*, Sep. 2016, pp. 193–199, doi:
        10.1109/ICELMACH.2016.7732526.
[32]   S. Huang, J. Zhang, J. Gao, and K. Huang, "Optimization the electromagnetic torque ripple of permanent magnet synchronous
        motor," in *2010 International Conference on Electrical and Control Engineering*, Jun. 2010, pp. 3969–3972, doi:
        10.1109/iCECE.2010.967.
[33]   Z. Chen, C. Xia, Q. Geng, and Y. Yan, "Modeling and analyzing of surface-mounted permanent-magnet synchronous machines
        with optimized magnetic pole shape," *IEEE Transactions on Magnetics*, vol. 50, no. 11, pp. 1–4, Nov. 2014, doi:
        10.1109/TMAG.2014.2327138.
[34]   Y. Li, J. Xing, T.Wang, and Y. Lu, "Programmable design of magnet shape for permanent-magnet synchronous motors with
        sinusoidal back EMF waveforms," *IEEE Transactions on Magnetics*, vol. 44, no. 9, pp. 2163–2167, Sep. 2008, doi:
        10.1109/TMAG.2008.2000750.
[35]   H. Vu Xuan, D. Lahaye, H. Polinder, and J. A. Ferreira, "Improved model for design of permanent magnet machines with
        concentrated windings," in *2011 IEEE International Electric Machines and Drives Conference (IEMDC)*, May 2011,
        pp. 948–954., doi: 10.1109/IEMDC.2011.5994943.

BIOGRAPHIES OF AUTHORS

Mustafa Yaseen Bdewi [iD] [SC] [P] received the B.Sc. degree in Electrical Engineering from University of Anbar, Iraq in 2012. He received the M.Sc. degree in Electrical Power Engineering from University of Technology, Iraq in 2020. His research interest includes finite element analysis and electrical machines design. He can be contacted at email: 316539@student.uotechnology.edu.iq.

Mohammed Moanes Ezzaldean Ali [iD] [SC] [P] received the B.Sc., M.Sc. and Ph.D. degrees in electrical engineering from University of Technology, Iraq in 1994, 1997 and 2009, respectively. In 1997, he joined the Research and Development Department-Al-Duha Electrical Industries Company Ltd. After that he was an Assistant Lecturer at Poly-Technique Higher Institute-Surman, Libya from 2001 to 2004. Mohammed Moanes was a consultant at the General Company for Electrical Industries-Baghdad from 2004 to 2006. Since May 2006, he has been with the Department of Electrical Engineering-University of Technology, where he was an Assistant Lecturer, became a Lecturer in 2009, and an Assistant Professor in 2018. His current research interests include induction heating, electrical machines and drives. He can be contacted at email: mohammedmoanes.e.ali@uotechnology.edu.iq.

Ahmed Mahmood Mohammed [iD] [SC] [P] received the B.Sc. and M.Sc. degrees from the University of Technology, Baghdad, Iraq, in 1994 and 2005, respectively, both in electrical and electronic engineering. He received his Ph.D. degree in electrical engineering at The University of Nottingham, Nottingham, U.K. in 2017. His research interests include high-power density electrical machines design, electromagnetic actuators, and material characterization of electrical machines. He can be contacted at email: ahmed.m.mohammed@uotechnology.edu.iq.